IFUSP/P-107

SEMIMICROSCOPIC DESCRIPTION OF THE ODD IODINE NUCLEI IN THE MASS REGION $123 \leq A \leq 133$

by

A. Szanto de Toledo, M.N. Rao, O. Sala

Instituto de Física, Universidade de São Paulo ,
São Paulo, Brasil

and

F. Krmpotić(x)

Departamento de Física, Facultad de Ciencias Exactas,
Universidad Nacional de La Plata, C.C.
Argentina

and

Instituto de Física, Universidade de São Paulo ,
São Paulo, Brasil.

(x) Member of the Carrera del Investigador Científico, Consejo Nacional de Investigaciones Científicas y Técnicas, Argentina.

SEMIMICROSCOPIC DESCRIPTION OF THE ODD IODINE NUCLEI IN THE MASS REGION $123 \leq A \leq 133$.

A.Szanto de Toledo, M.N. Rao, O. Sala.

Instituto de Física,Universidade de São Paulo,São Paulo, Brasil

and

F. Krmpotić[x]

Departamento de Física, Facultad de Ciencias Exactas,Universidad Nacional de La Plata, C.C. 67, Argentina

and

Instituto de Física,Universidade de São Paulo, São Paulo, Brasil.

---

[x] Member of the Carrera del Investigador Científico, Consejo Nacional de Investigaciones Científicas y Técnicas, Argentina.

ABSTRACT

A systematic study of the low-energy properties of odd-mass I nuclei is performed in terms of the Alaga model. Previous theoretical works are made up-to-date, according to the present level of experimental information, and extended to lighter isotopes. The residual interaction among the valence protons is approximated by both the pairing force and the surface delta interaction. We conclude that the refinements introduced by the last interaction are of little importance in the description of low energy states. Excitation energies, one-body reaction amplitudes, dipole and quadrupole moments and B(M1) and B(E2) values are calculated and compared with the corresponding experimental data. Also, a few allowed β-transitions are briefly discussed.

I. INTRODUCTION

Nuclei with a few valence protons (≤ 3) either below or above the Z=50 closed shell have been extensively studied, within the framework of the particle-phonon coupling scheme[1-8]. In this semi-microscopic model the Pauli principle is taken into account for the extra core protons (shell-model cluster), while the neutron valence shell, which is widely open, is described in terms of collective variables. When the shell-model cluster contains three particles, the particle-phonon coupling model is often referred to as the Alaga model.[9]

The coexistence of shell-model and collective features seems to be dominant in creating the properties of odd-mass I nuclei, and, a few years ago, the Alaga model was applied to ^{127}I by Paar[7], to ^{129}I by Vanden Berghe[8] and to ^{129}I and ^{131}I by Almar et al.[6] Since then, quite a bit of additional experimental data have been accumulated: i) Coulomb excitation in ^{127}I and ^{129}I has been studied by Renwick et al.[10]; ii) very detailed γ-decay studies on ^{129}I, ^{131}I and ^{133}I have been presented by the Livermore group[11,12]; iii) anisotropies in the γ-decay of oriented nuclei have been reported by Silverans et al.[13] for ^{129}I and by Lhersonneau et al.[14] for ^{131}I; iv) directional correlations of γ-rays in ^{129}I and ^{131}I have been performed by De Raedt et al.[15] and by Ludington et al.[16], respectively; and v) quite recently, the (^{3}He,d) reactions to $^{123, 125}$I have been measured by the São

Paulo group.[17] In view of this situation a new attempt has been made in the present work to explain, in a systematic way, the properties of low-energy states in odd-mass I isotopes from A=123 to A=133, within the Alaga framework. It should be noted that the above-mentioned theoretical studies[6-8], in addition to being limited to isolated nuclei, differ in several important aspects, namely: 1) while Paar[7] and Almar et al.[6], approximated the residual interaction by a pairing force (PF), Vanden Berghe[8] used the surface delta interaction (SDI); 2) the protons were distributed among four single-particle levels: 2 $d_{5/2}$, 1 $g_{7/2}$, 3 $s_{1/2}$ and 2 $d_{3/2}$ in Refs. 7 and 9, while in Ref. 6 the single-particle state 1 $h_{11/2}$ was also considered; and 3) the cut-off energies for the configuration space were not uniform.

In order to inquire to which extent the theoretical results are sensitive to the details of the residual interaction, the calculations were done with both the PF and the SDI.

II. NUCLEAR MODEL AND PARAMETERS

Since a detailed description of the model can be found in the literature[5-9, 18-21], only the main formulae are presented here.

The model Hamiltonian is:

$$H = H_{coll} + H_{sp} + H_{int} + H_{res} , \qquad (1)$$

where:

i) H_{coll} describes the harmonic quadrupole field of the Sn core;

ii) H_{sp} is associated with the motion of the three valence shell protons in an effective spherical potential;

iii) H_{int} represents the interaction energy between the three-particle cluster and the vibrational field and is given by the expression

$$H_{int} = -\frac{\beta}{\sqrt{5}} \sum_{\mu=-2}^{2} \left[b_2^{\mu\dagger} + (-)^{\mu} b_2^{-\mu} \right] \sum_{p} K(r_p)\, Y_{2\mu}^{*}(\theta_p, \phi_p). \qquad (2)$$

Here, $b_2^{\dagger}$ (b) is the creation (destruction) operator of the vibrational field, $K(r) = r \frac{dV}{dr}$ is the coupling strength and β is the quadrupole deformation parameter, related to the reduced transition probability in the core nucleus through the relation

$$B(E2;\ 0^+ \rightarrow 2^+) = \left(\frac{3}{4\pi} ZeR_o^2 \right)^2 \beta^2 \qquad (3)$$

iv) H_{res} is the residual interaction energy among the protons in the valence-shell cluster. The matrix elements of this two-body interaction are expressed in the form

$$\langle (j_1, j_2)\, J_{12} \,|H_{res}|\, (j_1', j_2')\, J_{12}' \rangle$$

$$= -\frac{G}{2} \frac{H(j_1\, j_2;\, J_{12})\, H(j_1'\, j_2';\, J_{12}')}{\left[(1+\delta_{j_1 j_2})\ (1+\delta_{j_1' j_2'}) \right]^{1/2}} \left[1 + (-)^{\ell_1' + \ell_2' + J_{12}} \right] \qquad (4)$$

where

$$H(j_1 j_2;\ J_{12}) = (2j_2 + 1)^{1/2}\ (j_2\ -1/2\ \ J_{12}0 \mid j_1\ -1/2)\ (-)^{\ell_2} \qquad (5a)$$

for the SDI[22], and

$$H(j_1 j_2;\ J_{12}) = (2j_1 + 1)^{1/2}\ (-)^{\ell_2}\ \delta_{j_1 j_2}\ \delta_{J_{12}0} \qquad (5b)$$

for the PF. The symbols $j_i \equiv (n_i,\ l_i,\ j_i)$ represent the quantum numbers of the proton states; $|(j_1,\ j_2)\ J_{12}>$ is an antisymetrized normalized wave function with angular momentum $\underset{\sim}{J}_{12} = \underset{\sim}{j}_1 + \underset{\sim}{j}_2$ and with the particles occupying the single-particle orbits j_1 and j_2.

The basis vectors of the total Hamiltonian for the states in odd-mass iodine nuclei, with angular momentum quantum number I and for the ground state in even-mass Te nuclei are, respectively

$$|\{(j_1,\ j_2)\ J_{12},\ j_3\}\ J;\ N\ R,\ I> \equiv |x_3,\ I>$$

and

$$|(j_1,\ j_2)\ J_{12};\ N\ R,\ O> \equiv |x_2,\ O>\ ,$$

where $\underset{\sim}{J} = \underset{\sim}{J}_{12} + \underset{\sim}{j}_3$ is the angular momentum of the three-proton cluster and $\underset{\sim}{R}$ ($\underset{\sim}{J} + \underset{\sim}{R} = \underset{\sim}{I}$) is the angular momentum of the N-phonon state. The corresponding eigenfunctions read

$$|I_n> = \sum_{x_3} \eta_3\ (x_3,\ I_n)\ \ |x_3,\ I>$$

and

$$|O_1> = \sum_{x_2} \eta_2 (x_2, O_1) \quad |x_2, O>$$

respectively, where the subindex n distinguishes between states of same angular momentum.

The spectroscopic factor for forming the state $|I_n>$ transfering a particle to the orbit j of the target state $|O_1>$ is given by

$$S_j(I_n) \equiv |< I_n \,||\, a_j^\dagger \,||\, O_1 >|^2 \, (2I + 1)^{-1}$$

$$= \left[\sum_{x_2', x_3} \left(\frac{2J + 1}{(2j+1)\ (2R+1)} \right)^{1/2} \eta_2(x_2', O_1) \ \eta_3(x_3, I_n) \right.$$

$$\left. x \ \theta_j (J_{12}', J) \ \delta_{RR'} \ \delta_{NN'} \ \delta_{R'J_{12}'} \right]^2 \qquad (6)$$

where

$$\theta_j(J_{12}', J) = <\{(j_1\ j_2)\ J_{12}, j_3\}\ J \,||\, a_j^\dagger \,||\, (j_1'\ j_2')\ J_{12}> \ (2J+1)^{-1/2} \qquad (7)$$

is the shell-model parentage coefficient.

The average number $<p>_j$ of protons in the (nlj) orbit of the target nucleus is defined as

$$<p>_j = \sum_{x_2} \left[\eta_2(x_2, O_1) \right]^2 \ (\delta_{jj_1} + \delta_{jj_2}) \ , \qquad (8)$$

and the resulting sum-rule limit is given by

$$\sum_n S_j(O_l, I_n) = 1 - \frac{\langle p \rangle_j}{2j+1} \quad . \tag{9}$$

The electric-quadrupole and magnetic-dipole operators consist of a particle and a collective part

$$M(E2,\mu) = e_p^{eff} \sum_i r_i^2 \; Y_2^\mu (\theta_i,\phi_i) + \frac{3R_0^2}{4\pi} \; e_v^{eff} \left[b_2^{\mu\dagger} + (-)^\mu \, b_2^{-\mu} \right] \tag{10}$$

$$M(M1,\mu) = \left(\frac{3}{4\pi}\right)^{1/2} \left[g_R \, R_\mu + g_\ell \, L_\mu + g_s \, S_\mu \right] \mu_N \tag{11}$$

where e_p^{eff} is the effective proton charge, $e_v^{eff} = Ze\beta/\sqrt{5}$ is the effective vibrator charge and g_R, g_ℓ and g_s are, respectively, the collective, orbital and spin gyromagnetic ratios. The B(E2) and B(M1) values are given by

$$B(\lambda;\, I_i \rightarrow I_f) = \frac{|\langle I_f || M(\lambda) || I_i \rangle|^2}{(2I_i + 1)} \tag{12}$$

where the reduced matrix elements $\langle I_f || M(\lambda) || I_i \rangle$ are defined as in Ref. 23.

The mixing ratio for the E2 and M1 transitions is calculated by the relation[24],

$$\delta = 8.33 \times 10^{-3} \, E_\gamma \, \frac{\langle I_f || M(E2) || I_i \rangle}{\langle I_f || M(M1) || I_i \rangle} \tag{13}$$

where $E_\gamma = E_i - E_f$ is the transition energy in MeV and the reduced matrix elements of the operators M(E2) and M(M1) are given in

units of e fm^2 and μ_N, respectively. This mixing ratio is related to that of Rose and Brink[25] by $\delta = -\delta_{RB}$.

We describe the states of iodine isotopes as belonging to the configurations with three protons distributed among the single particle states: $1g_{7/2}$, $2d_{5/2}$, $3s_{1/2}$, $2d_{3/2}$ and $1h_{11/2}$ and coupled to zero, one and two quadrupole phonons.

Our starting point in the choice of the model parameters was based on the previous works on odd-mass Sb and I nuclei[1, 5-8] and even-mass Te nuclei[4]. The final values, however, were determined by requiring a fit to certain experimental data, namely, the energies of the low states and the corresponding spectroscopic factors. Once the parameters occuring in the model are chosen, we calculate the electromagnetic properties.

The size of the configuration space was fixed by the condition:

$$\varepsilon(j_1)+\varepsilon(j_2)+\varepsilon(j_3)+N\hbar\omega \leq \begin{cases} 3 \text{ MeV} & \text{for } J_{12} \neq 0 \\ 3 \text{ MeV} + \frac{G}{2}(2J_{12}+1) & \text{for } J_{12} = 0 \text{ and } j_1 \neq 1h_{11/2} \\ 6 \text{ MeV} & \text{for } J_{12} = 0 \text{ and } j_1 = 1h_{11/2} \end{cases}$$

where the phonon energy $\hbar\omega$ = 1.15 MeV, the pairing constant G = 0.15 MeV and the single-particle energies $\varepsilon(j)$ were taken to be 0, 0.5, 1.8, 1.8 and 1.55 MeV for the orbitals $1g_{7/2}$, $2d_{5/2}$, $3s_{1/2}$, $2d_{3/2}$ and $1h_{11/2}$, respectively. In this way we still have reasonable dimensions for the energy matrices while retaining the most important basis states.

Parameters used in the calculations discussed in this paper are summarized in Table I. Values for the phonon energies $\hbar\omega$ of the core vibrations were chosen close to the experimental energies of the first excited 2^+ states in the neighbouring Sn isotopes. It should be noted that the single particle energies $\varepsilon(d_{5/2})$, $\varepsilon(d_{3/2})$, $\varepsilon(s_{1/2})$ and $\varepsilon(h_{11/2})$ increase with the mass number. The same effect was observed in the particle-phonon model calculations for odd-mass Sb and even-mass Te nuclei[1,4]. For the radial part of the particle-phonon interaction we have taken the fixed value $\langle K \rangle = 50$ MeV, which corresponds to the estimate from Ref. 23. In this way the measure of the vibrational field with the valence particles is mainly given by the effective deformation parameter β, which is related to the coupling strength "a", used in previous calculations[6,7] by

$$a = \frac{\langle K \rangle \beta}{\sqrt{20\pi}}$$

The values of β which we need here in order to reproduce the low-lying energy spectra of ^{123}I, ^{125}I and ^{127}I are appreciably larger than the ones used in the calculation of odd-mass Sb nuclei. This fact is mainly due to the truncation of the configuration space which we are obliged to perform here. Numerical calculations show that when the dimension of the configuration space increases, maintaining the same parametrization, the low-lying states become more collective; that is, their energy spectrum is more compressed, the quadrupole moments are larger, etc.

The coupling strength G, used in the present work for

the residual energy among the extra-core protons, agrees with the Kisslinger and Sorensen estimate[26].

The electromagnetic properties were evaluated with the usual values for the effective electric charge and the effective gyromagnetic ratios, namely

$$e_p^{eff} = e \text{ and } e_p^{eff} = 2e;$$

$$g_\ell = 1,\ g_s = 0.7 g_s^{free};$$

$$g_R = 0 \text{ and } g_R = Z/A.$$

III. RESULTS AND DISCUSSION

We shall limit our attention mainly to the positive parity states, due to fact that the interaction of the valence protons with the octupole vibrations as well with the negative parity non-collective states in the core nuclei should affect significantly the properties of the negative parity states in the odd iodine nuclei. The state $11/2_1^-$ is discussed merely in connection with the proton-transfer reaction data[17,27].

The results of the calculations for the low-lying states performed with the SDI and PF are very similar to each other. Therefore, the complete results will be presented only for the PF.

a) Energy spectra and spectroscopic factors

The experimental and calculated level schemes as well as the corresponding spectroscopic amplitudes are compared in Figs. 1-6. In order to be consistent in the DWBA analyses for all the iodine isotopes, the (^{3}He,d) angular distribution data of Auble et al.[27] for $^{127, 129, 131}$I were reanalysed with the code DWUCK[28].

In tables IIa and IIb are listed the wave functions calculated with the PF, for a few low-lying states in $^{123-133}$I and for the 0^+ ground states of the even-even $^{122-132}$Te nuclei, respectively.

The energies of the states below 1 MeV in excitation are, in general, well reproduced for both pairing and surface delta interactions. In particular, the model is able to explain the systematic lowering of the $5/2^+_1$, $3/2^+_1$ and $1/2^+_1$ states with decreasing mass number A. The energies of the $9/2^+_1$ and $11/2^+_1$ states based on the zero-phonon cluster $(g_{7/2})^3J$ are also well reproduced in all the nuclei in which these states have been observed.

Above 1 MeV excitation energy, the one-to-one identification of the experimental and calculated energies of the positive parity states turns out to be, in general, quite difficult and uncertain. Most of these states, and in particular those with $I^\pi \leq 7/2^+$, are very sensitive to the limitation of the configuration

space and the details of the residual interaction among the valence particles. Therefore, we refer briefly here only to some high spin states in ^{131}I. The levels with spins and parities of $11/2^+$, $15/2^+$ and $13/2^+$, observed at about 1.6 MeV excitation energy through E1 γ-feeding, may tentatively be identified with the calculated $11/2^+_3$ or $11/2^+_4$, $15/2^+_2$ and $13/2^+_2$ states, respectively. A possible explanation of the fact that the $13/2^+_1$,$15/2^+_1$ and $11/2^+_2$ states, predicted by the model, are not fed from odd-parity levels, could be atributed to the shell-model $\Delta j = 2$ forbiddenness. It should be noted that when only the single-particle states in the major shell Z=50 are considered, the E1 transitions are strictly forbidden. The existence of these transitions must be explained necessarily in terms of the admixtures from the neigbouring major shells.

The energy of the $11/2^-$ state is satisfactorily reproduced only for the ^{129}I, ^{131}I and ^{133}I nuclei. For the lighter isotopes the observed energy of this state is significantly lower than the predicted one, in spite of the fact that we have used a very low value for the single particle energy $\varepsilon(h_{11/2})$. It is to be realized that our parametrization for this single particle state might be somewhat artificial due to the facts that: i) the truncation of the configuration space excludes all the seniority three cluster states $(h_{11/2})^3 J$ and ii) the non-inclusion of the negative parity excitation modes of the core.

The states $7/2^+_1$, $5/2^+_1$, $5/2^+_2$, $3/2^+_1$, $1/2^+_1$ and $11/2^-_1$,are

the most relevant in connexion with the one-particle reaction process Te(^{3}He,d)I. In zeroth order approximation their basis vectors and the spectroscopic factors are:

$7/2^+_1$: $|\{(g_{7/2})^3\}\ 7/2;\ 00;\ 7/2\ >$ $\qquad S = \sqrt{3/4};$

$5/2^+_1$: $|\{(g_{7/2})^2\ \ 0,d\ 5/2\}\ 5/2,\ 00;\ 5/2\ >$ $\qquad S = 1;$

$5/2^+_2$: $|\{(g_{7/2})^3\}\ 5/2;\ 00;\ 5/2\ >$ $\qquad S = 0:$

$3/2^+_1$: $|\{(g_{7/2})^3\}\ 3/2;\ 00;\ 3/2\ >$ $\qquad S = 0;$

$1/2^+_1$: $|\{(g_{7/2})^2\ \ 0,d\ 5/2\}\ 5/2,\ 12;\ 1/2\ >$ $\qquad S = 0;$

$11/2^+_1$: $|\{(g_{7/2})^2\ \ 0,h\ 11/2\}\ 11/2,\ 00;\ 11/2\ >$ $\qquad S = 1.$

The residual interaction with G ≈0.2 affects only the spetroscopic strengths for the states $7/2^+_1$, $5/2^+_1$ and $11/2^-_1$, resulting in $S(7/2^+_1) \approx 0.8$, $S(5/2^+_1) \approx 0.9$ and $S(11/2^-_1) \approx 0.7$. On introducing a weak cluster-field interaction (β≈0.05) this situation essentially persists (see the calculated results for ^{133}I in Fig.6). For a moderate particle-phonon interaction (β≈0.12 or a ≈0.6MeV), the single-particle strength is significantly removed from the states $7/2^+_1$, $5/2^+_1$ and $11/2^-_1$, while the states $3/2^+_1$ and $1/2^+_1$ receive appreciable spectroscopic strengths. The largest part of the $d_{5/2}$ strength is shifted into the $5/2^+_2$ states. When the cluster-field interaction is increased still more to a value of β≈0.14 or a ≈0.9, the wave functions of the low-lying states are strongly mixed with pronounced collective character, which is

reflected in a still larger reduction of the spectroscopic strengths. This situation corresponds to the model prediction for the lighter iodine isotopes, namely ^{123}I and ^{125}I. Partial contributions of the first four $1/2^+$, $3/2^+$, $5/2^+$ and $7/2^+$ states in ^{127}I described in the present model calculation by a moderate coupling, are displayed in Table III. Except for the $7/2^+_2$, $7/2^+_4$ and $3/2^+_4$ states the partial zero-phonon spectroscopic amplitudes are coherent among themselves. In most cases the one-phonon contributions are quite significant, while those which arise from two-phonons are always very small. States with small collective contribution to the spectroscopic factor come from incoherent addition of small terms.

There is a reasonable over all agreement between the experimental and calculated spectroscopic factors. However, it should be pointed out that, in going from the heavier to the lighter I isotopes, the theory predicts a systematic decrease in the reaction amplitudes for the $7/2^+_1$ and $5/2^+_1$ states, which is not observed experimentally. However, the measured (^{3}He,d) absolute cross sections for the $7/2^+_1$ levels have large (~30%) experimental uncertainties[17]. Also, the absolute spectrocospic factors calculated with the DWBA theory could be uncertain by as much as 30%. In view of these facts it might be premature to consider this discrepancy a serious failure of the model.

The theoretical and experimental results for the summed spectroscopic strenghts up to an excitation energy of 2.5 MeV are compared in Table IV, which also presents the predicted sum-rule

limits. The calculated results for the $2d_{3/2}$ and $3s_{1/2}$ transition strengths are consistently lower than those observed experimentally. This discrepancy could be attributed to the truncation of the configuration space which affects mostly the $s_{1/2}$ and $d_{3/2}$ single-particle strengths, spread out in many high-lying levels.

b) Electromagnetic Properties

An extensive calculation of the electromagnetic properties of odd-mass I nuclei was performed in order to study their variation in going from ^{123}I to ^{133}I. We also hope that the results presented below could be used as a guide to experimenters for future measurements. The main component of the wave functions, which were used in the evaluation of the electromagnetic operators M(E2) and M(M1) are listed in Table IIa. The moments and transitions probabilities for ^{123}I, ^{127}I and ^{131}I are presented in Tables V and VI, respectively. We thought it unnecessary to show the results for ^{125}I and ^{129}I as most of them fall in between the corresponding results for the neighboring nuclei.

Before comparing the calculated results with experiment, we discuss briefly the electromagnetic properties in the framework of the cluster-field model. When only the first order effects are included, the quadrupole moment for a predominantly particle state is enhanced due to the collective effects, i.e.,

$$Q(J) = Q^{p}(J)\, e^{eff} \qquad (14)$$

where $e\,Q^p(J)$ is the bare quadrupole moment of the cluster and

$$e^{eff} = e_p^{eff} + \frac{\langle K \rangle \beta^2 Ze}{2\pi \hbar\omega} \qquad (15)$$

Given below are the zeroth-order approximations for some low-lying states and the corresponding quadrupole moments as obtained from the relation (14) for ^{131}I with $e_p^{eff} = e$ ($e^{eff} = 3.34\ e$):

$7/2^+_1 : |\{(g_{7/2})^3\}\ 7/2,\ 00;\ 7/2 >,$ $\quad Q = -0.17$ eb

$5/2^+_1 : |\{(g_{7/2})^2\ \ 0,d\ 5/2\}\ 5/2,\ 00;\ 5/2 >,$ $\quad Q = -0.42$ eb

$5/2^+_2 : |\{(g_{7/2})^3\}\ 5/2,\ 00;\ 5/2 >,$ $\quad Q = -0.46$ eb

$3/2^+_1 : |\{(g_{7/2})^3\}\ 3/2,\ 00;\ 3/2 >,$ $\quad Q = \ \ 0.30$ eb

$9/2^+_1 : |\{(g_{7/2})^3\}\ 9/2,\ 00;\ 9/2 >,$ $\quad Q = \ \ 0.23$ eb

$11/2^+_1 : |\{(g_{7/2})^3\}11/2,\ 00;\ 11/2 >,$ $\quad Q = -0.05$ eb

$15/2^+_1 : |\{(g_{7/2})^3\}15/2,\ 00;\ 15/2 >,$ $\quad Q = -0.37$ eb

$13/2^+_1 : |\{(g_{7/2})^2\ \ 4,d\ 5/2\}\ 13/2,\ 00;\ 13/2 >,$ $\quad Q = -0.40$ eb

Comparing these quadrupole moments with the ones diplayed in Table V, which shows the results of the exact calculations, one can see that the expression (14) takes into account the most important effects in building up the quadrupole moment of the $7/2^+_1$, $5/2^+_1$, $5/2^+_2$, $3/2^+_1$, $15/2^+_1$ and $13/2^+_1$ states. It is to be noted that the quadrupole moment of the $7/2^+_1$ is relatively small due to the Pauli principle. The quadrupole moments of the $11/2^+_1$ and $9/2^+_1$ states are higher-order effects. The first one arises essentially

from the admixture of the broken pair $|\{(g_{7/2})^2\ 6,d\ 3/2\}\ ;\ J = 11/2 >$. In the latter case the cluster $|\{(g_{7/2})^2\ 2,d\ 5/2\}\ ;\ 9/2;\ J = 9/2 >$ competes destructively with the basis state $|\{(g_{7/2})^3\}\ 9/2,\ J = 9/2 >$ for a moderate coupling, and dominates when the coupling is incresead , resulting in a negative quadrupole moment.

Most of the E2 transitions among the low-lying states in zeroth-order are of the particle type N=0,ΔN=0. In this situation, the transition moment $<J_f||\ r^2\ Y_2||\ J_i>$ is renormalized by the effective charge,

$$e_1^{eff} = e_p^{eff} + \frac{<K>\ \beta^2\ Ze}{2\pi} \quad \frac{\hbar\omega}{(\hbar\omega)^2 - (\varepsilon_{J_i} - \varepsilon_{J_f})^2} \qquad (16)$$

where ε_{J_i} and ε_{J_f} are the energies of the cluster in the initial and final states, respectively. Then, if the transition energy between the participating clusters is smaller than the phonon energy, the foregoing transition moment is enhanced. However, when $<J_f||\ r^2\ Y_2||\ J_i >$ is relatively small due to the Pauli principle or spin-flip, this picture may break down and the transition in this case is dominated by the contributions from the higher-lying multiplet states of the same spin. Characteristic N=0, ΔN=0 E2 transitions are $3/2^+_1 \rightarrow 7/2^+_1$, $11/2^+_1 \rightarrow 7/2^+_1$ and $11/2^+_1 \rightarrow 15/2^+_1$. Examples of spin-flip transitions are, $7/2^+_1 \rightarrow 5/2^+_1$, $9/2^+_1 \rightarrow 5/2^+_1$, $3/2^+_1 \rightarrow 5/2^+_1$ and $5/2^+_2 \rightarrow 5/2^+_1$. In the case of the $7/2^+_1 \rightarrow 5/2^+_1$ transition, the process occurs dominantly through the moment $<\{(g_{7/2})^3\}\ 7/2||\ r^2\ Y_2||\{\ (g_{7/2})^3\}\ 5/2 >$. The transition $5/2^+_2 \rightarrow$

$7/2^+_1$ is also of the type N=0, ΔN=0, but it is somewhat reduced due to the incoherent contribution which arises from the moment $<(g_{7/2})^3\ 7/2||\ r^2\ Y_2||\{(g_{7/2})^2\ 0,d\ 5/2\},\ 5/2>$. The B(E2; $1/2^+_1 \rightarrow 5/2^+_1$) is an example of a characteristic ΔN=1, N=1 $\rightarrow$ N=0 multiplet-to-cluster transition.

The magnetic properties, in general, do not change considerably in going from isotope to isotope. It is worth noting that for the $7/2^+_1$ state, the contributions to the magnetic moment from both the orbital and the spin parts are very close to the single-particle estimates. Expressing the reduced matrix elements as

$$< I_i||\ M(M1)||\ I_f > = (g_R\ C + g_\ell\ D + g_s\ E)\ \mu_N$$

in the case of ^{131}I, we have:

$$D = 5.88,\ D_{sp} = 6.10;\ E = 0.56,\ E_{sp} = 0.61.$$

On the other hand, the spin contribution to the dipole moments of the $5/2^+_1$ and $3/2^+_1$ states are significantly reduced by the cluster-phonon interaction. The numerical results for the above-mentioned nucleus are:

$D = 2.97,\ D_{sp} = 2.83;\ E = 0.35,\ E_{sp} = 0.71$, for the state $5/2^+_1$,

and

$D = 2.22,\ D_{sp} = 2.27;\ E = 0.11,\ E_{sp} = 0.38$, for the state $3/2^+_1$.

The collective contributions to the dipole moments of the low-lying states are of comparatively little size. This statement is also

valid for most of the B(M1) transitions. The ℓ-forbiddenness in B(M1; $7/2^+_1 \rightarrow 5/2^+_1$) and B(M1; $3/2^+_1 \rightarrow 1/2^+_1$) is removed largely through the one-phonon admixtures.

The available experimental data on the electric quadrupole and magnetic dipole moments[29], and the B(E2) and B(M1) transition probabilities[10, 30-35] are presented and compared with the calculated values for the iodine isotopes in Table VII. For ^{123}I and ^{131}I the experimental transition moments were derived from the observed half-lives, using the measured values of E2/M1 mixing ratios and branchings. The total conversion coefficients used in deriving the moments were obtained from the Internal Conversion Tables[36]. The experimental data are fairly well reproduced and the only discrepancy which deserves being mentioned is the one related with the $3/2^+_1 \rightarrow 5/2^+_1$ M1 transition. This is a highly retarded transition; for example, in ^{125}I the measured B(M1) value is only 1/120 of the Moszkowski single-particle estimate. The calculated value, which arises from a strong cancellation effect between the orbital part ($g_\ell D = 0.23$) and the spin part ($g_s E = -0.31$), is very sensitive to the choice of the effective gyromagnetic ratio g_s^{eff}. Clearly, in such a situation some higher order effects as, for example, the contributions of the velocity dependent potentials might also be important.

The calculated mixing ratios δ are compared in Table VIII with the available experimental quantities[13-16, 37-40]. With the exceptions of the $1/2^+_1 \rightarrow 3/2^+_1$ and $7/2^+_2 \rightarrow 7/2^+_1$ transitions

in ^{127}I and the $9/2^+_2 \rightarrow 7/2^+_1$ transition in ^{131}I, there is a good agreement between theory and experiment both for the signs and for the magnitudes of the mixing ratios. It should be noted however that the measured mixing ratios for the foregoing transitions in ^{127}I have opposite signs compared to those in the neighboring ^{125}I and ^{129}I isotopes.

c) Allowed β-transitions

We finish this section with a few words on the allowed Gamow-Teller transitions. The low-lying states and, in particular the $5/2^+_1$ and $5/2^+_2$ states, exhibit an inverse relationship between the spectroscopic factors and the ft-values. This fact, of course, is not surprising, as both processes take place mainly through the zero-phonon seniority-one components in the final states. A simple qualitative relation is obtained if we build up the wave functions of the $3/2^+_1$ state in the odd-mass Te nucleus, from the ground-state wave function of the even-mass Te nucleus, by coupling to it a quasiparticle in the $2d_{3/2}$ orbit, namely if

$$|\mathrm{Te};\ 3/2^+_1> \equiv |\mathrm{Te};\ 0^+_1>|\ n,\ d_{3/2}>.$$

In this approximation we have

$$|<I_n||\underset{\sim}{\sigma}\ t_-||\mathrm{Te};\ 3/2^+_1>|^2 = S_j(I_n)\,|<J||\underset{\sim}{\sigma}\ t_-||\ n,\ d_{3/2}>|^2\ U^2(d_{3/2}), \tag{17}$$

where $J = I$, $\underset{\sim}{\sigma} \equiv 2\underset{\sim}{s}$ and $U(d_{3/2})$ is the occupation probability of the $d_{3/2}$ neutron state. The operator t_- transforms a neutron into

a proton. The desired relation is

$$\frac{S_j(I_n)}{S_j(I_n')} = \left| \frac{\langle I_n || \underset{\sim}{\sigma}\, t_- || \mathrm{Te};\ 3/2^+_1 \rangle}{\langle I_n' || \underset{\sim}{\sigma}\, t_- || \mathrm{Te};\ 3/2^+_1 \rangle} \right|^2 = \frac{ft(I_n')}{ft(I_n)} \qquad (18)$$

In the expression (17) the anharmonicities induced by the interaction of the two protons with the tin core are taken into account. However, we neglect both the coupling energy between the quasineutron and the Te core and the residual proton-neutron energy. While the former effect seems to be of little importance[41], the latter one is very significant as the particle-hole charge-exchange correlations strongly renormalize the single-particle moments $\langle j || \underset{\sim}{\sigma}\, t_- || j' \rangle$ [42,43].

The estimate (18) was tested for the $5/2^+_1$ and $5/2^+_2$ states, which have rather large amplitudes $|\{(j)^2\ 0, d_{5/2}\}\ 5/2; 00\rangle$ in the corresponding wave functions. The results for the ratio $S_{5/2}(5/2^+_1)/\ S_{5/2}(5/2^+_2)$, as obtained from the experimental ft-values and Eq. (18), are presented in Table IX (second column) and confronted with the (^{3}He,d) measurements (third column), as well as, with theoretical values (fourth column).

SUMMARY AND CONCLUSIONS

The properties of the odd-mass iodine nuclei, in the mass-region $123 \leq A \leq 133$, were calculated within the framework

of the three-particle cluster core coupling model. All available data on the energy spectra, one-body reaction strengths, electric and magnetic moments and B(E2) and B(M1) values were examined. It was possible to give a reasonably accurate description of these observables using a uniform set of single particle energies. However, further experimental data are needed on ^{123}I and ^{125}I before a more detailed comparison can be made.

The results reported here indicate that the coupling energy between the three-particle cluster and the quadrupole vibration field, together with the residual interaction between the promoted pairs ($J_{12} = 0$), play a decisive role in establishing the structure of the low-lying states. The residual interaction between broken pairs ($J_{12} \neq 0$) affects in an appreciable way only the states above ~1 MeV, where the effects of correlations and excitation modes not included in the present approach are also important. It seems then reasonable to approximate the residual interaction with the PF, as was actually done in most of the previous calculations[3,5-7,9].

ACKNOWLEFGMENT

One of us (F.K.) wishes to thank the University of São Paulo for the kind hospitality he found during his stay there.

REFERENCES

1. G. Vanden Berghe and K. Heyde, Nucl. Phys. A163, 478 (1971).
2. S.M. Abecasis, O. Civitarese and F. Krmpotić, Phys. Rev. C9, 2320 (1974).
3. G.Alaga, F. Krmpotić and V. Lopac, Phys. Lett. 24B, 537 (1967).
4. E. Degrieck and G. Vanden Berghe, Nucl. Phys. A231, 141 (1974).
5. O. Civitarese and F. Krmpotić, Nucl. Phys. A229, 133 (1974).
6. R. Almar, O. Civitarese and F. Krmpotić, Phys. Rev. C8, 1518 (1973).
7. V. Paar, Nucl. Phys. A211, 29 (1973).
8. G. Vanden Berghe, Z.Phys. 266, 139 (1974).
9. G. Alaga, Bull. Am. Phys. Soc. 4, 359 (1959); G. Alaga and G. Ialongo, Nucl. Phys. A97; 600 (1967).
10. B.W. Renwick, B. Byrne, D.A. Eastham, P.D. Forsyth and D.G.E. Martin, Nucl. Phys. A208, 574 (1973).
11. S.V. Jackson, UCRL-51846 (Ph. D. Thesis), (1975): S.V. Jackson, W.B. Walters and R.A. Meyer, Phys. Rev. C11, 1323 (1975).
12. L.G. Mann, W.B. Walters and R.A. Meyer, UCRL-77984 (1976).
13. R.E. Silverans, E. Schoeters and L. Vanneste, Nucl. Phys. A204 , 625 (1973).
14. G. Lhersonneau; J. De Raedt, H. Van de Voorde, H.Ooms, R. Haroutunian, E. Schoeters, R.E. Silverans and L. Vanneste, Phys. Rev. C12, 609 (1975).

15. J. de Raedt, M. Rots and H. Van de Voorde, Phys. Rev. C9 , 2391 (1974).

16. M.A. Lundington, P.L. Gardulski and H. L. Wiedenbeck, Phys. Rev. C11, 987 (1975).

17. A. Szanto de Toledo, M. N. Rao, N. Ueta and O. Sala, Phys. Rev. (to be published).

18. G. Alaga, in Cargese Lectures in Theorical Physics, Edited by M. Lévy (Gordon and Breach, N.Y. 1968), vol. II; in Nuclear Structure and Nuclear Reactions, Proceedings of the International School of Physics "Enrico Fermi", Course 40 , edited by M. Jean and R. A. Ricci (Academic, N.Y., 1969).

19. G. Alaga, F. Krmpotić, V. Paar and L. Šips, Rudjer Bošković Institute Reports No. IRB-TP-7-70 and IRB-TP-4-73.

20. R. Almar, O. Civitarese, F. Krmpotić and J. Navaza, Phys. Rev. C6, 187 (1972).

21. V. Paar, Heavy-ion, High-spin states and Nuclear Structure (IEAA, Vienna 1975), vol. II, p. 179.

22. A. Plastino, R. Arvieu and S.A. Moszkowski, Phys. Rev. 145, 837 (1966).

23. A. Bohr and B.R. Mottelson, Nuclear Structure, (Benjamin , New York, 1969), vol. I; ibid. vol. II, to be published.

24. K.S. Krane and R.M. Steffen, Phys. Rev. C2, 724 (1970).

25. H.J. Rose and D.M. Brink, Rev. Mod. Phys. 39, 306 (1967).

26. L.S. Kisslinger and R.A. Sorensen, Rev. Mod. Phys. 35, 853 (1963).

27. R.L. Auble, J.B. Ball and C.B. Fulmer, Phys. Rev. 169, 955

(1968). We thank Dr. R.L. Auble for furnishing the (^{3}He,d) angular distribution data.

28. P.D. Kunz, University of Colorado (1967), unpublished.
29. G.H. Fuller and V.W. Cohen, Nucl. Data A5, 433 (1969).
30. R.L. Auble, Nucl. Data Sheets, B7, 363 (1972).
31. J. Kownacki, J. Ludziejewski and M. Moszynski, Nucl. Phys. A107, 1176 (1968).
32. A.G. Svensson, R.W. Sommerfeldt, L.O. Norlin and P.N. Tandon, Nucl. Phys. A95, 653 (1967).
33. J.S. Geiger, R.L. Graham, I. Bergstrom and F. Brown, Nucl. Phys. 68, 352 (1965).
34. R.H. Davis, A.S. Divatia, D.A. Lind and R.D. Moffat, Phys.Rev. 103, 1801 (1956).
35. E.S. Macias and W.B. Walters, Nucl. Phys. A161, 471 (1971).
36. R.S. Hager and E.C. Seltzer, Nucl. Data A4, 1 (1968).
37. R.L. Auble, Nuclear Data Sheets B7, 465 (1972).
38. J.S. Geiger, Phys. Rev. 158, 1094 (1967).
39. R.L. Auble, Nuclear Data Sheets B8, 77 (1972).
40. C.E. Bemis and K. Fransson, Phys. Lett. 19, 567 (1965).
41. R.E. Silverans, R. Coussement, E. Schoeters and L. Vanneste, Nucl. Phys. A202, 467 (1973).
42. J.A. Halbleib and R.A. Sorensen, Nucl. Phys. A98, 542 (1967).
43. L. Szybisz, F. Krmpotić and M.A. Fariolli, Phys. Rev. C9, 624 (1974).

Table I: Parameters used in the present calculations.

	^{123}I	^{125}I	^{127}I	^{129}I	^{131}I	^{133}I
$\varepsilon(g_{7/2})$ (MeV)	0.00	0.00	0.00	0.00	0.00	0.00
$\varepsilon(d_{5/2})$ (MeV)	0.15	0.20	0.30	0.35	0.45	0.50
$\varepsilon(s_{1/2})$ (MeV)	1.00	1.15	1.45	1.90	2.35	2.90
$\varepsilon(d_{3/2})$ (MeV)	1.10	1.20	1.30	1.60	2.00	2.65
$\varepsilon(h_{11/2})$ (MeV)	1.00	1.00	1.00	1.10	1.55	1.90
$\hbar\omega$ (MeV)	1.10	1.15	1.15	1.15	1.15	1.20
β	0.143	0.140	0.120	0.105	0.080	0.050
G (pairing) (MeV)	0.15	0.15	0.15	0.15	0.15	0.175
G (S.D.I.) (MeV)	0.20	0.20	0.20	0.20	0.20	0.225

Table II a. Calculated Wave Functions of a low-lying states in $^{123-125}I$ nuclei. Only amplitudes larger than 4 are listed.

	^{123}I	^{125}I	^{127}I	^{129}I	^{131}I	^{133}I
$1/2_1^+$						
$\|\{(g\ 7/2)^2\ 0,d\ 5/2\}\ 5/2;\ 12\ >$	- 0.533	- 0.537	- 0.557	- 0.596	- 0.640	- 0.684
$\|\{(g\ 7/2)^2\ 2,d\ 5/2\}\ 1/2;\ 00\ >$	0.235	0.243	0.263	0.308	0.406	0.526
$\|\{(g\ 7/2)^2\ 0,s\ 1/2\}\ 1/2;\ 00\ >$	- 0.499	- 0.496	- 0.483	- 0.436	- 0.366	- 0.242
$\|\{(g\ 7/2)^2\ 2,d\ 5/2\}\ 9/2;\ 24\ >$	0.226	0.223	0.214	0.212	0.193	
$\|\{(g\ 7/2)^2\ 2,s\ 1/2\}\ 5/2;\ 12\ >$	0.253	0.247	0.224			
$\|\{(g\ 7/2)^2\ 2,s\ 1/2\}\ 3/2;\ 12\ >$	0.202	0.199				
$3/2_1^+$						
$\|\{(g\ 7/2)^3\}\ 3/2;\ 00\ >$	0.372	0.388	0.415	0.458	0.560	0.685
$\|\{(g\ 7/2)^3\}\ 7/2;\ 12\ >$	- 0.410	- 0.416	- 0.440	- 0.465	- 0.496	- 0.541
$\|\{(g\ 7/2)^3\}\ 5/2;\ 12\ >$	- 0.244	- 0.248	- 0.245	- 0.249	- 0.246	- 0.171
$\|\{(g\ 7/2)^2\ 0,d\ 3/2\}\ 3/2;\ 00\ >$	- 0.321	- 0.318	- 0.317	- 0.300	- 0.243	
$\|\{(g\ 7/2)^2\ 2,d\ 3/2\}\ 3/2;\ 00\ >$	0.256	0.255	0.241	0.220		
$\|\{(d\ 5/2)^2\ 0,g\ 7/2\}\ 7/2;\ 12\ >$						- 0.212
$5/2_1^+$						
$\|\{(g\ 7/2)^2\ 0,d\ 5/2\}\ 5/2;\ 00\ >$	0.477	0.481	0.504	0.534	0.595	0.812
$\|\{(g\ 7/2)^3\}\ 5/2;\ 00\ >$	0.248	0.262	0.288	0.299	0.338	
$\|\{(g\ 7/2)^3\}\ 7/2;\ 12\ >$	0.228	0.238	0.258	0.266	0.290	
$\|\{(g\ 7/2)^2\ 0,d\ 5/2\}\ 5/2;\ 12\ >$	- 0.352	- 0.346	- 0.334	- 0.326	- 0.296	- 0.232
$\|\{(g\ 7/2)^2\ 2,d\ 5/2\}\ 7/2;\ 12\ >$	- 0.291	- 0.288	- 0.273	- 0.262	- 0.230	- 0.148
$\|\{(g\ 7/2)^2\ 2,d\ 5/2\}\ 5/2;\ 12\ >$	- 0.253	- 0.249	- 0.236	- 0.225	- 0.199	
$\|\{(g\ 7/2)^2\ 2,d\ 5/2\}\ 5/2;\ 00\ >$	0.254	0.253	0.239	0.228	0.195	
$\|\{(d\ 5/2)^3\}\ 5/2;\ 00\ >$						0.270
$\|\{(h11/2)^2\ 0,d\ 5/2\}\ 5/2;\ 00\ >$						- 0.210

Continued

Table IIa. Continued

$5/2_2^+$

$\|\{(g\ 7/2)^3\}\ 5/2;\ 00\ >$	0.438	0.465	0.514	0.555	0.602	0.732
$\|\{(g\ 7/2)^3\}\ 7/2;\ 12\ >$	0.355	0.369	0.397	0.414	0.409	0.496
$\|\{(g\ 7/2)^2\ 0,d\ 5/2\}\ 5/2;\ 00\ >$	- 0.233	- 0.250	- 0.289	- 0.317	- 0.389	- 0.220
$\|\{(g\ 7/2)^2\ 2,d\ 5/2\}\ 9/2;\ 12\ >$	0.234	0.217				
$\|\{(g\ 7/2)^2\ 2,d\ 3/2\}\ 3/2;\ 12\ >$	0.228	0.222	0.198			
$\|\{(g\ 7/2)^2\ 2,s\ 1/2\}\ 5/2;\ 00\ >$	0.221	0.187				
$\|\{(g\ 7/2)^3\}\ 3/2;\ 12\ >$	0.212	0.210	0.197			
$\|\{(g\ 7/2)^2\ 4,d\ 3/2\}\ 5/2;\ 00\ >$	0.203	0.194				
$\|\{(g\ 7/2)^2\ 0,d\ 5/2\}\ 5/2;\ 12\ >$			0.208	0.214	0.202	

$7/2_1^+$

$\|\{(g\ 7/2)^3\}\ 7/2;\ 00\ >$	- 0.513	- 0.534	- 0.596	- 0.643	- 0.739	- 0.822
$\|\{(d\ 5/2)^2\ 0,g\ 7/2\}\ 7/2;\ 00\ >$	- 0.240	- 0.240	- 0.258	- 0.282	- 0.307	- 0.394
$\|\{(g\ 7/2)^3\}\ 5/2;\ 12\ >$	0.245	0.249	0.254	0.252	0.240	
$\|\{(g\ 7/2)^3\}11/2;\ 12\ >$	0.257	0.261	0.263	0.255	0.235	
$\|\{(h11/2)^2\ 0,g\ 7/2\}\ 7/2;\ 00\ >$					0.180	0.227
$\|\{(g\ 7/2)^2\ 2,d\ 5/2\}\ 7/2;\ 00\ >$	0.249	0.241	0.201	0.176		
$\|\{(g\ 7/2)^2\ 0,d\ 5/2\}\ 5/2;\ 12\ >$	0.206	0.199				

$7/2_2^+$

$\|\{(g\ 7/2)^2\ 0,d\ 5/2\}\ 5/2;\ 12\ >$	0.314	0.318	0.345	0.365	0.387	0.378
$\|\{(g\ 7/2)^2\ 2,d\ 5/2\}\ 5/2;\ 12\ >$	0.323	0.327	0.336	0.334	0.317	0.209
$\|\{(d\ 5/2)^2\ 0,g\ 7/2\}\ 7/2;\ 00\ >$	0.235	0.228				
$\|\{(g\ 7/2)^2\ 2,d\ 5/2\}\ 7/2;\ 00\ >$	0.408	0.427	0.489	0.526	0.601	0.616
$\|\{(g\ 7/2)^2\ 6,d\ 5/2\}\ 7/2;\ 00\ >$	0.225	0.214				
$\|\{(g\ 7/2)^2\ 2,d\ 5/2\}\ 9/2;\ 12\ >$	- 0.203	- 0.210	- 0.235	- 0.238	- 0.238	
$\|\{(g\ 7/2)^3\}\ 7/2;\ 00\ >$			0.203	0.200		
$\|\{(g\ 7/2)^2\ 4,d\ 5/2\}\ 7/2;\ 00\ >$				0.205	0.218	
$\|\{(g\ 7/2)^3\}\ 7/2;\ 12\ >$						0.356

Continued

Table IIa. Continued

$9/2_1^+$

$\|\{(g\ 7/2)^2\ 0,d\ 5/2\}\ 5/2;\ 12\ >$	- 0.275	- 0.277	- 0.288	- 0.289	- 0.226	
$\|\{(g\ 7/2)^3\}\ 7/2;\ 12\ >$	- 0.201	- 0.207	- 0.237	- 0.265	- 0.341	- 0.443
$\|\{(g\ 7/2)^2\ 2,d\ 5/2\}\ 7/2;\ 12\ >$	0.309	0.309	0.301	0.288	0.220	
$\|\{(g\ 7/2)^2\ 2,d\ 5/2\}\ 9/2;\ 00\ >$	0.406	0.415	0.426	0.427	0.363	
$\|\{(g\ 7/2)^2\ 4,d\ 5/2\}13/2;\ 12\ >$	- 0.300	- 0.294	- 0.270	- 0.240		
$\|\{(g\ 7/2)^3\}\ 9/2;\ 00\ >$			0.218	0.294	0.522	0.765
$\|\{(g\ 7/2)^3\}11/2;\ 12\ >$					0.230	0.187
$\|\{(g\ 7/2)^2\ 4,d\ 5/2\}\ 9/2;\ 00\ >$	0.247	0.252	0.256	0.253	0.200	

$11/2_1^+$

$\|\{(g\ 7/2)^3\}\ 7/2;\ 12\ >$	0.387	0.392	0.415	0.438	0.461	0.497
$\|\{(g\ 7/2)^3\}\ 11/2;\ 00\ >$	- 0.496	- 0.514	- 0.557	- 0.596	- 0.678	- 0.759
$\|\{(g\ 7/2)^2\ 4,d\ 5/2\}\ 11/2;\ 00\ >$	0.224	0.220	0.201	0.192		
$\|\{(g\ 7/2)^2\ 6,d\ 3/2\}\ 11/2;\ 00\ >$	- 0.227	- 0.220	- 0.201	- 0.165		
$\|\{(g\ 7/2)^3\}\ 15/2;\ 12\ >$	0.271	0.274	0.275	0.269	0.253	0.184

$13/2_1^+$

$\|\{(g\ 7/2)^2\ 4,d\ 5/2\}\ 13/2;\ 00\ >$	0.352	0.369	0.419	0.487	0.593	0.743
$\|\{(g\ 7/2)^2\ 6,d\ 5/2\}\ 13/2;\ 00\ >$	0.274	0.283	0.310	0.342	0.393	0.459
$\|\{(g\ 7/2)^2\ 6,s\ 1/2\}\ 13/2;\ 00\ >$	- 0.343	- 0.331	- 0.290	- 0.256		
$\|\{(g\ 7/2)^2\ 6,s\ 1/2\}\ 13/2;\ 12\ >$	0.211	0.201				
$\|\{(g\ 7/2)^2\ 6,d\ 5/2\}\ 17/2;\ 12\ >$	- 0.444	- 0.443	- 0.435	- 0.414	- 0.354	- 0.232
$\|\{(g\ 7/2)^2\ 2,d\ 5/2\}\ 9/2;\ 12\ >$			- 0.210	- 0.235	- 0.246	- 0.197

Continued

Table II a. Continued

$15/2_1^+$

$\|\{(g\ 7/2)^3\}\ 11/2;\ 12>$	- 0.330	- 0.333	- 0.338	- 0.339	- 0.318	- 0.225
$\|\{(g\ 7/2)^2\ 6,d\ 3/2\}\ 11/2;\ 12>$	- 0.236	- 0.229	- 0.212			
$\|\{(g\ 7/2)^2\}\ 15/2;\ 00>$	0.598	0.619	0.677	0.721	0.816	0.932
$\|\{(g\ 7/2)^2\ 6,d\ 5/2\}\ 15/2;\ 00>$	- 0.265	- 0.259	- 0.227	- 0.222		
$\|\{(g\ 7/2)^3\}\ 15/2;\ 12>$	- 0.253	- 0.252	- 0.247	- 0.242	- 0.220	
$\|\{(g\ 7/2)^2\ 6,d\ 5/2\}\ 15/2;\ 12>$	0.209	0.203				

$11/2^-$

$\|\{(g\ 7/2)^2\ 0,h\ 11/2\}\ 11/2;\ 00>$	- 0.704	- 0.710	- 0.738	- 0.765	- 0.814	- 0.857
$\|\{(g\ 7/2)^2\ 0,h\ 11/2\}\ 11/2;\ 12>$	0.341	0.338	0.323	0.307	0.271	0.185
$\|\{(d\ 5/2)^2\ 0,h\ 11/2\}\ 11/2;\ 00>$	- 0.191	- 0.192	- 0.215	- 0.231	- 0.263	- 0.353
$\|\{(g\ 7/2)^2\ 2,h\ 11/2\}\ 11/2;\ 00>$	- 0.326	- 0.321	- 0.282	- 0.247	- 0.187	
$\|\{(h11/2)^3\}\ 11/2;\ 00>$	0.169	0.173	0.193	0.205	0.185	0.213
$\|\{(g\ 7/2)^2\ 2,h\ 11/2\}\ 11/2;\ 12>$	0.281	0.277	0.252	0.229	0.190	
$\|\{(g\ 7/2)^2\ 2,h\ 11/2\}\ 13/2;\ 12>$	0.254	0.251	0.234	0.218		

Table IIb: Calculated wave functions for the 0^+ ground states of $^{122-132}Te$ nuclei. Only amplitudes larger than 4% are listed.

	^{122}Te	^{124}Te	^{126}Te	^{128}Te	^{130}Te	^{132}Te
$\|(g\ 7/2)^2\ 0;\ 00>$	0.595	0.618	0.667	0.706	0.774	0.823
$\|(d\ 5/2)^2\ 0;\ 00>$	0.397	0.383	0.363	0.361	0.356	0.405
$\|(g\ 7/2)^2\ 2;\ 12>$	-0.369	-0.380	-0.379	-0.374	-0.344	-0.217
$\|(g\ 7/2,\ d\ 3/2)\ 2;\ 12>$	0.276	0.272	0.254	0.220		
$\|(d\ 5/2)^2\ 2;\ 12>$	-0.217	0.201				
$\|(h11/2)^2\ 0;\ 00>$			-0.221	-0.234	-0.220	-0.255

Table III. Partial contributions of the ground state in ^{126}Te to the spectroscopic factors in ^{127}I. The columns labelled by I,II and III are respectively, the contributions from the dominant component $|(g\ 7/2)^2\ 0,00>$, that from all the zero - phonon states, and the total spectroscopic factor.

n	I	II	III
	$1/2^+$ states		
1	0.100	0.150	0.250
2	0.001	0.0013	0.0013
3	0.003	0.012	0.010
4	0.058	0.100	0.134
	$3/2^+$ states		
1	0.048	0.076	0.122
2	0.081	0.128	0.195
3	0.014	0.030	0.038
4	0.0002	0.0011	0.0008
	$5/2^+$ states		
1	0.113	0.156	0.345
2	0.037	0.052	0.104
3	0.019	0.031	0.054
4	0.033	0.057	0.087
	$7/2^+$ states		
1	0.119	0.224	0.409
2	0.014	0.041	0.054
3	0.022	0.003	0.012
4	0.0006	0.034	0.033

Table IV. Results for the summed spectroscopic strengths. The experimental and theoretical summed spectroscopic strengths are up to an excitation energy of 2.5 MeV.

Nucleus		SINGLE - PARTICLE LEVEL				
		1g 7/2	2d 5/2	2d 3/2	3s 1/2	1h 11/2
^{123}I	ΣS_{exp}	0.75	0.59	0.51	0.60	0.35
	ΣS_{th}	0.52	0. 59	0.32	0.36	0.33
	Sum-rule limit	0.85	0.92	0.96	0.97	0.99
^{125}I	ΣS_{exp}	0.51	0.64	0.99	0.63	0.60
	ΣS_{th}	0.53	0.60	0.34	0.37	0.41
	Sum-rule limit	0.84	0.93	0.96	0.97	0.99
^{127}I	ΣS^{*}_{exp}	0.59	0.70	0.72	0.75	0.50
	ΣS_{th}	0. 56	0.68	0.38	0.40	0.46
	Sum-rule limit	0.83	0.94	0.97	0.98	0.99
^{129}I	ΣS^{*}_{exp}	0.45	0.84	0.83	0.81	0.63
	ΣS_{th}	0.61	0.74	0.37	0.37	0.52
	Sum-rule limit	0.82	0.94	0.97	0.99	0.99
^{131}I	ΣS^{*}_{exp}	0.64	0.81	0.57	0.81	0.50
	ΣS_{th}	0.69	0.85	0.30	0.31	0.65
	Sum-rule limit	0.82	0.95	0.98	0.99	0.99

*Values obtained from the reanalysis of the data of Auble et al (Ref:27)

Table V . Calculated electric quadrupole and magnetic dipole moments, in units of eb and μ_N , respectively. Q_I, Q_{II} refer to $e_p^{eff} = e$ and $e_p^{eff} = 2e$, μ_I , μ_{II} refer to $g_R = 0$ and $g_R = Z/A$, respectively.

Level	^{123}I				^{127}I				^{131}I			
	Q_I	Q_{II}	μ_I	μ_{II}	Q_I	Q_{II}	μ_I	μ_{II}	Q_I	Q_{II}	μ_I	μ_{II}
$5/2_1$	-0.76	-0.94	3.08	3.18	-0.65	-0.83	3.04	3.13	-0.45	-0.62	3.09	3.15
$7/2_1$	-0.47	-0.58	2.51	2.61	-0.39	-0.50	2.41	2.49	-0.24	-0.34	2.34	2.38
$1/2_1$	–	–	1.95	1.85	–	–	1.95	1.84	–	–	1.87	1.74
$3/2_1$	0.26	0.34	1.17	1.06	0.23	0.31	1.20	1.08	o.18	0.27	1.24	1.11
$5/2_2$	-0.21	-0.26	2.27	2.31	-0.29	-0.37	2.18	2.23	-0.29	-0.39	2.23	2.27
$9/2_1$	-0.28	-0.35	4.10	4.33	-0.20	-0.26	3.96	4.20	0.00	0.00	3.38	3.60
$11/2_1$	-0.49	-0.62	3.55	3.81	-0.39	-0.51	3.46	3.72	-0.20	-0.30	3.37	3.62
$7/2_2$	-0.36	-0.45	2.83	3.04	-0.20	-0.26	3.28	3.49	-0.11	-0.16	3.62	3.81
$3/2_2$	-0.10	-0.09	-0.02	0.13	-0.20	-0.28	0.36	0.49	-0.17	-0.23	1.66	1.67
$5/2_3$	0.40	0.52	2.99	2.98	0.35	0.46	3.16	3.18	0.05	0.08	3.01	3.08
$7/2_3$	-0.36	-0.46	2.20	2.27	-0.49	-0.63	1.21	1.90	-0.43	-0.61	1.46	1.58
$3/2_3$	-0.05	-0.08	0.49	0.50	-0.12	-0.15	0.34	0.33	-0.07	-0.10	0.89	0.88
$9/2_2$	-0.46	-0.61	3.51	3.75	-0.34	-0.47	3.34	3.56	0.06	0.08	3.78	3.92
$13/2_1$	-0.72	-0.93	6.15	6.16	-0.61	-0.81	6.14	6.18	-0.37	-0.49	6.06	6.15
$1/2_2$	–	–	-0.02	0.11	–	–	0.04	0.12	–	–	0.39	0.43
$9/2_3$	0.04	0.05	3.22	3.43	0.05	0.06	3.40	3.64	-0.31	-0.45	3.23	3.62
$11/2_2$	-0.68	-0.87	2.95	3.17	-0.40	-0.52	3.76	3.94	-0.10	-0.13	4.42	4.55
$15/2_1$	-0.71	-0.90	5.20	4.92	-0.60	-0.77	4.90	5.17	-0.38	-0.53	4.89	5.06

Table VI . Transition Probabilites B(E2) in units of $e^2 10^{-50} cm^4$ and B(M1) in units of $\mu_N^2 \times 10^2$ for ^{123}, ^{127}, ^{131}I. The subscripts I and II have the same significance as in Table V .

Transition	^{123}I				^{127}I				^{131}I			
	B(E2) I	B(E2) II	B(M1) I	B(M1) II	B(E2) I	B(E2) II	B(M1) I	B(M1) II	B(E2) I	B(E2) II	B(M1) I	B(M1) II
$7/2_1 \rightarrow 5/2_1$	7.3	11.5	2.5	2.3	5.4	8.9	1.2	1.2	2.4	4.7	0.2	0.2
$5/2_1 \rightarrow 5/2_1$	3.3	5.3	7.4	7.7	2.8	4.9	6.9	7.7	1.4	2.9	2.9	4.2
$3/2_1 \rightarrow 7/2_1$	11.3	18.6	–	–	9.6	16.5	–	–	7.0	7.9	–	–
$1/2_1 \rightarrow 5/2_1$	9.7	15.6	–	–	7.5	12.7	–	–	6.3	10.9	–	–
$1/2_1 \rightarrow 3/2_1$	4.0	7.4	8.5	4.6	2.5	5.0	7.9	4.4	1.5	3.2	6.0	3.8
$5/2_2 \rightarrow 5/2_1$	0.4	0.5	14.9	15.2	0.4	0.6	21.2	22.1	0.1	0.2	27.1	28.1
$5/2_2 \rightarrow 7/2_1$	4.2	6.7	0.5	0.1	3.7	6.0	0.7	0.2	2.5	4.7	0.4	0.1
$5/2_2 \rightarrow 3/2_1$	4.1	7.0	11.0	7.1	2.6	4.6	7.5	4.3	1.9	3.5	5.1	2.7
$5/2_2 \rightarrow 1/2_1$	2.6	4.4	–	–	1.6	2.9	–	–	1.0	1.8	–	–
$11/2_1 \rightarrow 7/2_1$	9.9	15.4	–	–	8.0	13.0	–	–	6.5	11.0	–	–
$9/2_1 \rightarrow 5/2_1$	3.3	4.9	–	–	2.8	4.5	–	–	1.4	2.5	–	–
$9/2_1 \rightarrow 7/2_1$	5.8	8.8	7.4	5.4	3.9	6.2	5.3	3.9	2.0	3.4	1.5	0.9
$9/2_1 \rightarrow 5/2_2$	3.3	5.6	–	–	1.3	2.3	–	–	0.01	0.02	–	–
$9/2_1 \rightarrow 11/2_1$	1.2	1.8	5.5	3.8	1.5	2.5	4.6	3.1	1.8	3.5	2.3	1.1
$7/2_2 \rightarrow 5/2_1$	0.1	9.0	13.2	8.8	5.1	7.2	12.6	9.0	3.1	5.6	8.1	6.2
$7/2_2 \rightarrow 7/2_1$	0.4	0.6	9.5	12.3	0.03	0.04	6.8	8.8	0.04	0.1	2.0	2.7
$7/2_2 \rightarrow 5/2_1$	0.1	0.1	-	-	0.1	0.2	-	-	0.01	0.01	-	-
$7/2_2 \rightarrow 5/2_2$	0.2	0.3	0.1	0.1	1.1	1.7	0.1	0.03	0.8	1.4	0.7	0.4
$7/2_2 \rightarrow 11/2_1$	0.2	0.2	–	–	0.9	1.3	–	–	0.4	1.6	–	–
$7/2_2 \rightarrow 9/2_1$	1.8	2.8	27.4	26.2	3.0	5.1	25.7	21.1	1.6	3.3	14.9	30.9
$3/2_2 \rightarrow 5/2_1$	0.2	0.3	24.9	22.9	0.02	0.02	47.8	48.0	0.9	1.5	15.6	9.5
$3/2_2 \rightarrow 7/2_1$	0.0	0.0	–	–	0.1	0.2	–	–	0.4	0.6	–	–
$3/2_2 \rightarrow 3/2_1$	0.5	0.8	0.3	0.2	1.7	3.1	0.3	0.04	0.6	1.1	1.0	2.7
$3/2_2 \rightarrow 1/2_1$	4.1	7.1	1.6	0.8	2.2	4.2	2.4	1.3	0.5	1.0	28.0	19.7
$3/2_2 \rightarrow 5/2_2$	3.4	5.8	38.0	49.1	5.4	9.4	45.8	33.7	0.1	0.1	2.3	3.6
$3/2_2 \rightarrow 7/2_2$	2.7	4.3	–	–	0.03	0.04	–	–	0.2	0.5	–	–
$9/2_2 \rightarrow 5/2_1$	3.9	5.8	–	–	2.3	3.6	–	–	0.3	0.5	–	–
$9/2_2 \rightarrow 7/2_1$	1.0	1.6	3.3	3.6	1.3	2.0	0.8	1.5	0.02	0.03	1.0	0.8
$9/2_2 \rightarrow 5/2_2$	2.1	3.7	–	–	2.5	4.5	–	–	1.8	3.4	–	–
$9/2_2 \rightarrow 11/2_1$	4.4	7.3	0.4	0.0	3.3	5.7	1.2	0.2	0.3	0.6	0.8	0.6
$9/2_2 \rightarrow 9/2_1$	0.2	0.3	0.1	0.02	0.2	0.4	0.6	0.3	0.7	1.3	14.6	16.9
$9/2_2 \rightarrow 7/2_2$	1.2	1.9	1.3	2.6	0.4	0.6	0.8	1.5	1.2	2.3	13.3	11.8
$13/2_1 \rightarrow 11/2_1$	1.5	2.4	1.1	0.9	1.1	1.8	1.3	1.1	0.5	0.9	1.2	1.0
$13/2_1 \rightarrow 9/2_1$	1.9	3.3	–	–	4.5	7.7	–	–	1.5	2.9	–	–

Table VII . Comparison Between Experiment and Theory.
(The magnetic dipole and electric quadrupole moments are in units of μ_N and eb, respectively. The B(E2), B(M1) values are in units of $e^2\ 10^{-50}\ cm^4$ and $\mu_N^2 \times 10^2$, respectively. The simbols I and II have the same significance as in Table V .)

Nucleus	Quantity	Experiment	Theory	
			I	II
^{123}I	B(E2) ↓			
	$1/2^+_1 \rightarrow 5/2^+_1$	22.5 ± 0.3 [a]	9.7	15.6
	B(M1) ↓			
	$3/2^+_1 \rightarrow 5/2^+_1$	1.67 ± 0.10 [a]	7.4	7.7
	$5/2^+_2 \rightarrow 5/2^+_1$	25.0 ± 8.0 [a,b]	14.9	15.2
	$3/2^+_2 \rightarrow 5/2^+_1$		24.9	22.9
^{125}I	$\mu(5/2^+_1)$	+3.0 [c]	3.06	3.32
	$Q(5/2^+_1)$	-0.89 [c]	-0.74	-0.93
	B(E2) ↓			
	$7/2^+_1 \rightarrow 5/2^+_1$	4.44 ± 0.12 [d]	7.2	11.4
	$3/2^+_1 \rightarrow 5/2^+_1$	7.14 ± 0.30 [d]	3.3	5.5
	$1/2^+_1 \rightarrow 5/2^+_1$	12.30 ± 0.78 [d]	9.4	15.2
	$3/2^+_1 \rightarrow 7/2^+_1$	14.48 ± 0.40 [d]	11.3	18.7
	$1/2^+_1 \rightarrow 3/2^+_1$	1.88 ± 0.80 [d]	3.7	6.9
	B(M1) ↓			
	$7/2^+_1 \rightarrow 5/2^+_1$	2.80 ± 0.08 [d]	2.1	2.0
	$3/2^+_1 \rightarrow 5/2^+_1$	1.40 ± 0.04 [d]	6.7	7.1
	$1/2^+_1 \rightarrow 3/2^+_1$	9.72 ± 0.96 [d]	8.2	4.5
^{127}I	$\mu(5/2^+_1)$	+2.808 [c]	3.04	3.13
	$Q(5/2^+_1)$	-0.79 [c]	-0.65	-0.83
	$\mu(7/2^+_1)$	2.06 ± 0.15 [e]	2.41	2.49

continued

Table VII. Continued

^{127}I	$Q(7/2^+_1)$	-0.71[c]	-0.39	-0.50
	$\mu(3/2^+_1)$	0.96 ± 0.20[e]	1.20	1.08
	B(E2) ↓			
	$7/2^+_1 \rightarrow 5/2^+_1$	6.42 ± 1.02[d]	5.4	8.9
	$3/2^+_1 \rightarrow 5/2^+_1$	7.08 ± 1.32[d] 6.45 ± 0.75[f]	2.8	4.9
	$1/2^+_1 \rightarrow 5/2^+_1$	~ 7 [d] 8.1 ± 0.9 [f]	7.5	12.7
	$3/2^+_2 \rightarrow 5/2^+_1$	0.27 ± 0.06[f]	0.02	0.02
	$7/2^+_2 \rightarrow 5/2^+_1$	6.53 ± 0.9 [f]	5.1	8.0
	$9/2^+_1 \rightarrow 5/2^+_1$	1.56 ± 0.18[f]	2.8	4.5
	$9/2^+_2 \rightarrow 5/2^+_1$	7.20 ± 0.72[f]	2.3	3.6
	$3/2^+_1 \rightarrow 7/2^+_1$	11.20 ± 0.24[d]	9.6	16.5
	$1/2^+_1 \rightarrow 3/2^+_1$	<4[d]	2.5	5.1
	B(M1) ↓			
	$7/2^+_1 \rightarrow 5/2^+_1$	2.36 ± 0.12[g]	1.2	1.2
	$3/2^+_1 \rightarrow 5/2^+_1$	0.72 ± 0.04[d]	6.9	7.7
	$1/2^+_1 \rightarrow 3/2^+_1$	~8.6[h]	7.9	4.4
^{129}I	$\mu(7/2^+_1)$	2.617[c]	2.38	2.44
	$Q(7/2^+_1)$	-0.55[c]	-0.34	-0.45
	$\mu(5/2^+_1)$	2.8[c]	3.07	3.14
	$Q(5/2^+_1)$	-0.68[c]	-0.58	-0.76
	B(E2) ↓			
	$3/2^+_1 \rightarrow 7/2^+_1$	7.0 ± 0.8 [f]	7.9	14.0
	$5/2^+_1 \rightarrow 7/2^+_1$	2.13 ± 0.4 [f]	3.3	5.6
	$11/2^+_1 \rightarrow 7/2^+_1$	8.13 ± 0.87[f]	6.5	11.0
	$9/2^+_1 \rightarrow 7/2^+_1$	6.24 ± 0.64[f]	3.2	5.1
	$7/2^+_2 \rightarrow 7/2^+_1$	1.1 ± 0.4 [f]	0.3	0.3
	$3/2^+_2 \rightarrow 7/2^+_1$	0.8 ± 0.4 [f]	0.3	0.4
	$9/2^+_2 \rightarrow 7/2^+_1$	1.2 ± 0.24[f]	1.0	1.6
	$7/2^+_3 \rightarrow 7/2^+_1$	0.8 ± 0.3 [f]	1.8	2.6

continued

Table VII. Continued

^{131}I	$\mu(7/2^+_1)$	2.74[c]	2.34	2.38
	$Q(7/2^+_1)$	-0.40[c]	-0.24	-0.34
	B(E2) ↓			
	$5/2^+_1 \rightarrow 7/2^+_1$	7.07 ± 0.47[i]	2.4	4.7
	B(M1) ↓			
	$5/2^+_1 \rightarrow 7/2^+_1$	1.09 ± 0.07[i]	0.2	0.2

a) ref. 30
b) The measured half-life refers to the 0.33-MeV level.
c) ref. 29 d) ref. 31 e) ref. 32 f) ref. 10
g) ref. 33 h) ref. 34 i) ref. 35

Table VIII. Comparision of experimental and theoretical mixing ratios. δ_I and δ_{II} refer to $e_p^{eff} = e$ and $e_p^{eff} = 2e$, respectively. The effective gyromagnetic ratios are $g_R = 0$, $g_\ell = 1$ and $g_s^{eff} = 0.7\ g_s^{free}$ in both cases.

Nucleus	Transition	δ (Exp)	δ_I	δ_{II}
^{125}I	$1/2_1^+ \rightarrow 3/2_1^+$	$-0.08 > \delta > -1.5$ [a] $\lvert\delta\rvert = 0.02 \pm 0.1$ [b]	-0.020	-0.026
	$7/2_1^+ \rightarrow 5/2_1^+$	-0.02 ± 0.04 [a] $\lvert\delta\rvert = 0.12 \pm 0.02$ [b]	-0.16	-0.21
	$3/2_1^+ \rightarrow 5/2_1^+$	0.32 ± 0.07 [a]	0.14	0.19
^{127}I	$7/2_1^+ \rightarrow 5/2_1^+$	-0.086 ± 0.005 [c]	-0.046	-0.046
	$1/2_1^+ \rightarrow 3/2_1^+$	0.08 ± 0.02 [c]	-0.07	-0.09
	$3/2_1^+ \rightarrow 5/2_1^+$	0.52 ± 0.05 [c]	0.12	0.12
	$5/2_2^+ \rightarrow 7/2_1^+$	-0.18 ± 0.03 or -2.5 ± 0.2 [c]	1.0	1.8
	$5/2_2^+ \rightarrow 3/2_1^+$	$0.21 \pm 0.04, < -26, > 47$ [c]	0.16	0.21
	$5/2_2^+ \rightarrow 5/2_1^+$	$\lvert\delta\rvert = 0.077 \pm 0.010$ [c]	0.066	0.064
	$5/2_1^+ \rightarrow 7/2_1^+$	-0.053 ± 0.014 [d]	-0.057	-0.058
	$3/2_1^+ \rightarrow 5/2_1^+$	$0.53^{+0.16}_{-0.12}$ or $3.5^{+2.0}_{-1.1}$ [e]	0.15	0.14

Continued

Table VIII. Continued

^{129}I	$5/2_2^+ \rightarrow 3/2_1^+$	-0.22 ± 0.05 [e]	-0.10	-0.14
	$1/2_1^+ \rightarrow 3/2_1^+$	-0.08 ± 0.03 or 2.09 ± 0.14 [e]	-0.08	-0.11
	$5/2_2^+ \rightarrow 7/2_1^+$	$0.50\ ^{+0.17}_{-0.10}$ [f]	0.98	1.71
	$5/2_2^+ \rightarrow 5/2_1^+$	$-0.076^{+0.037}_{-0.048}$ [f]	-0.048	-0.047
	$9/2_1^+ \rightarrow 7/2_1^+$	-0.34 ± 0.06 [f]	-0.56	-0.66
^{131}I	$5/2_1^+ \rightarrow 7/2_1^+$	-0.33 ± 0.12 [g]	-0.52	-0.45
	$5/2_2^+ \rightarrow 5/2_1^+$	-1.1 ± 1.3 [g]	-0.02	-0.02
	$9/2_1^+ \rightarrow 7/2_1^+$	-1.20 ± 0.09 or $-0.580^{+0.049}_{-0.057}$ [h]	-0.77	-0.96
	$9/2_2^+ \rightarrow 7/2_1^+$	$1.2^{+0.9}_{-0.5}$ [h]	-0.11	-0.12

a) Ref. 37 b) Ref. 38 c) Ref. 39 d) Ref. 40

e) Ref. 15 f) Ref. 13 g) Ref. 16 h) Ref. 14.

Table IX. Results for the ratio $S_{5/2}(5/2_1) / S_{5/2}(5/2_2)$:

I) estimates obtained from Eq.(18) and the experimental ft-values;

II) results from the (^{3}He,d) measurements; and

III) theoretical values calculated with the PF.

Nucleus	I	II	III
^{127}I	4.9	4.4	3.5
^{129}I	2.0	2.7	2.8
^{131}I	1.3	1.2	2.4

FIGURE CAPTION

Experimental and calculated level schemes and spectroscopic amplitudes for:

1) $^{123}_{I}$

2) $^{125}_{I}$

3) $^{127}_{I}$

4) $^{129}_{I}$

5) $^{131}_{I}$

6) $^{133}_{I}$

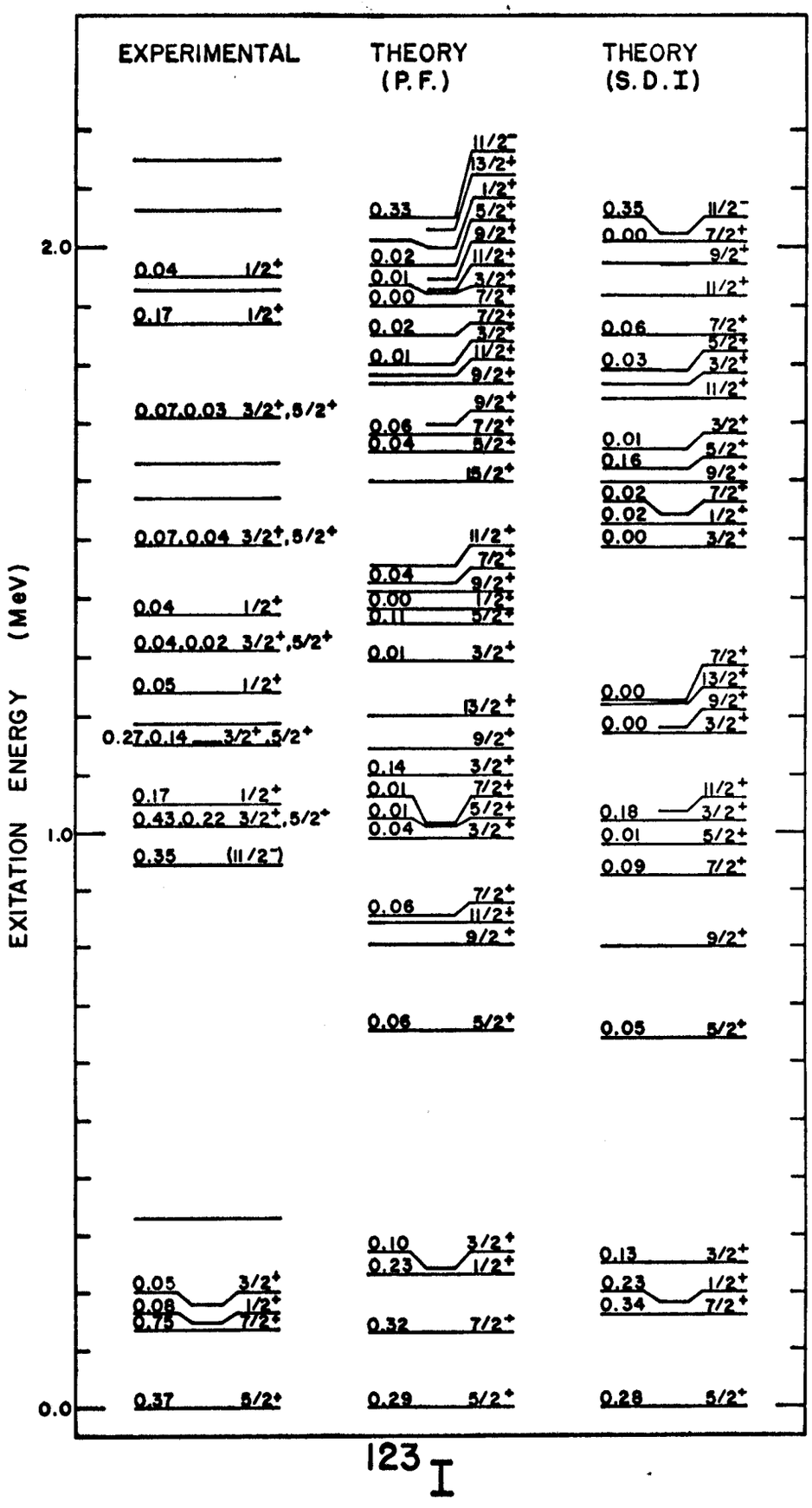
EXPERIMENTAL
THEORY (P.F.)
THEORY (S.D.I)
EXITATION ENERGY (MeV)
2.0
1.0
0.0
0.04 1/2+
0.17 1/2+
0.07,0.03 3/2+,5/2+
0.07,0.04 3/2+,5/2+
0.04 1/2+
0.04,0.02 3/2+,5/2+
0.05 1/2+
0.27,0.14 3/2+,5/2+
0.17 1/2+
0.43,0.22 3/2+,5/2+
0.35 (11/2-)
0.05 3/2+
0.08 1/2+
0.75 7/2+
0.37 5/2+
0.33 11/2-
13/2+
1/2+
5/2+
9/2+
0.02 11/2+
0.01 3/2+
0.00 7/2+
0.02 7/2+
3/2+
0.01 11/2+
9/2+
9/2+
0.06 7/2+
0.04 5/2+
15/2+
11/2+
7/2+
0.04 9/2+
0.00 1/2+
0.11 5/2+
0.01 3/2+
13/2+
9/2+
0.14 3/2+
0.01 7/2+
0.01 5/2+
0.04 3/2+
0.06 7/2+
11/2+
9/2+
0.06 5/2+
0.10 3/2+
0.23 1/2+
0.32 7/2+
0.29 5/2+
0.35 11/2-
0.00 7/2+
9/2+
11/2+
0.06 7/2+
0.03 5/2+
3/2+
11/2+
0.01 3/2+
0.16 5/2+
9/2+
0.02 7/2+
0.02 1/2+
0.00 3/2+
7/2+
0.00 13/2+
9/2+
0.00 3/2+
11/2+
0.18 3/2+
0.01 5/2+
0.09 7/2+
9/2+
0.05 5/2+
0.13 3/2+
0.23 1/2+
0.34 7/2+
0.28 5/2+
123 I

FIGURE 1

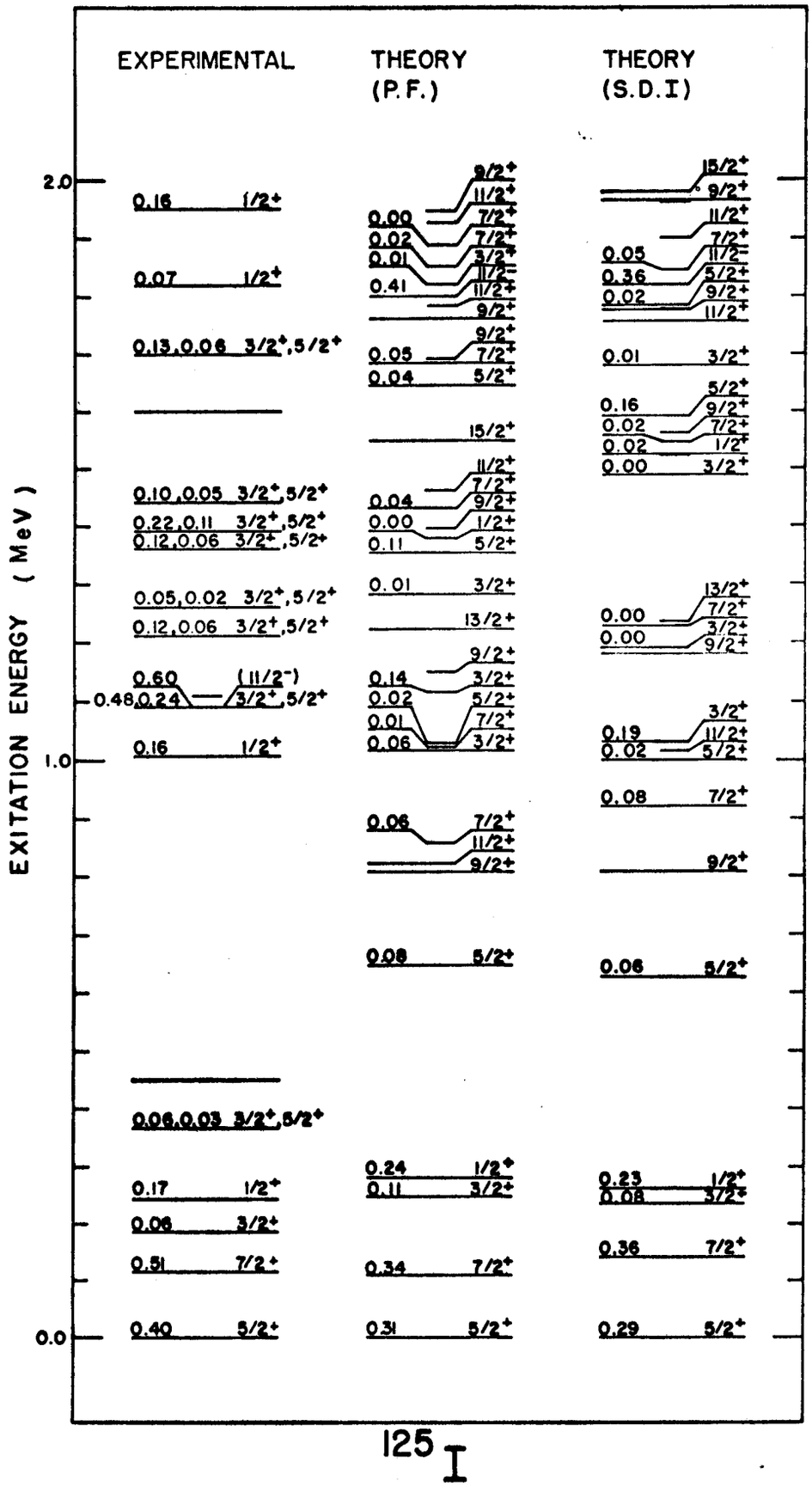

^{125}I

FIGURE 2

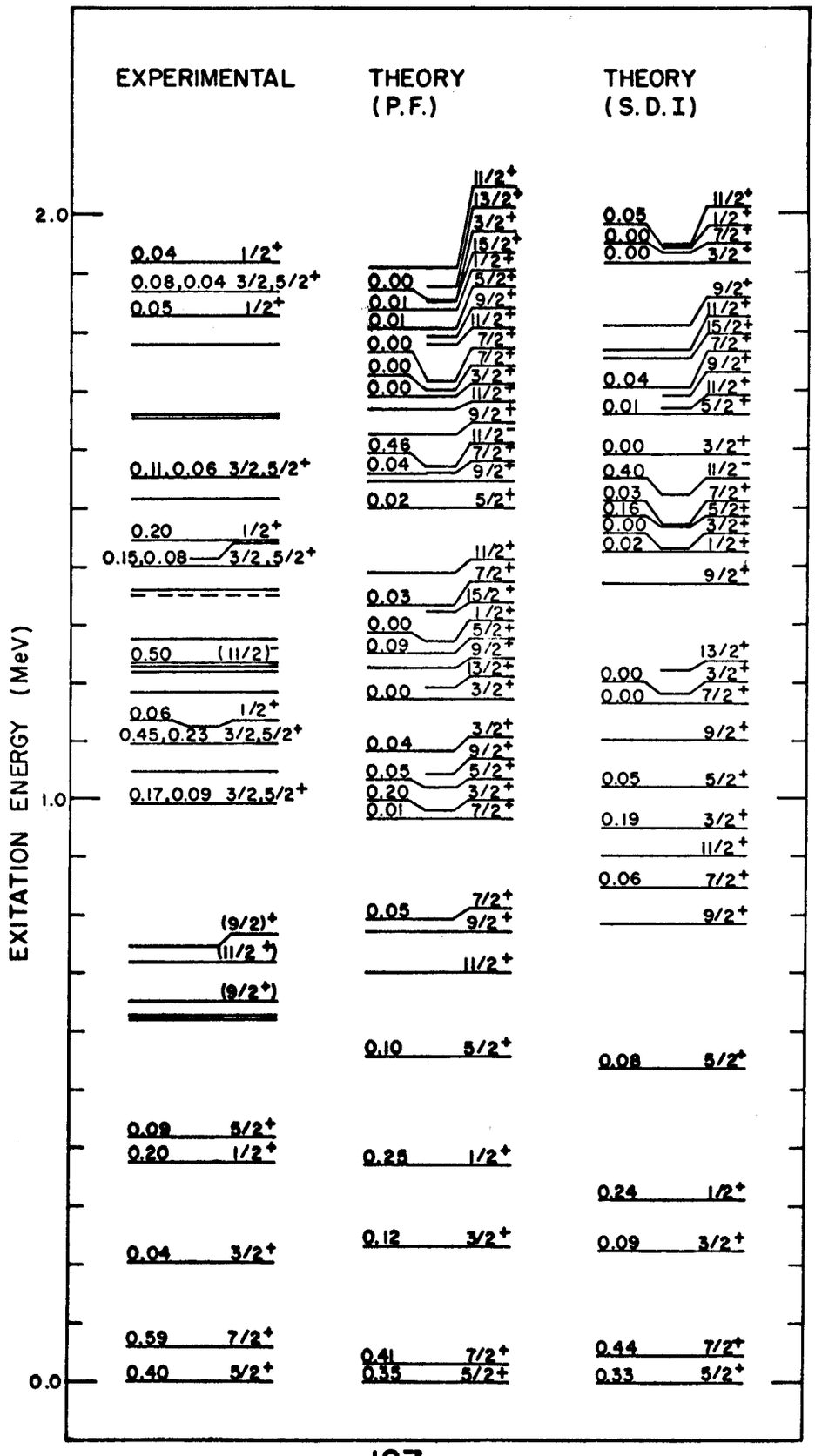

$^{127}_{53}I$

FIGURE 3

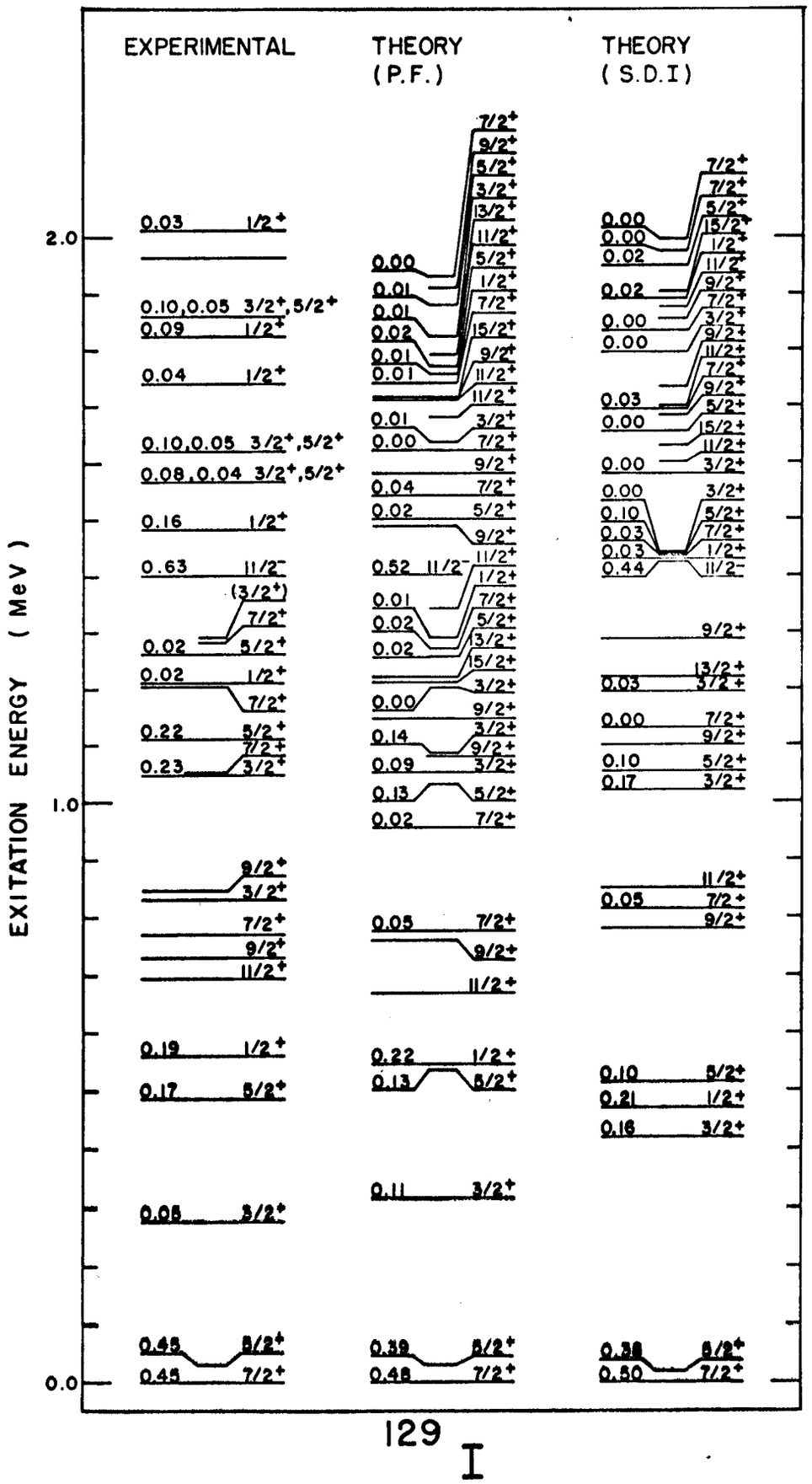

^{129}I

FIGURE 4

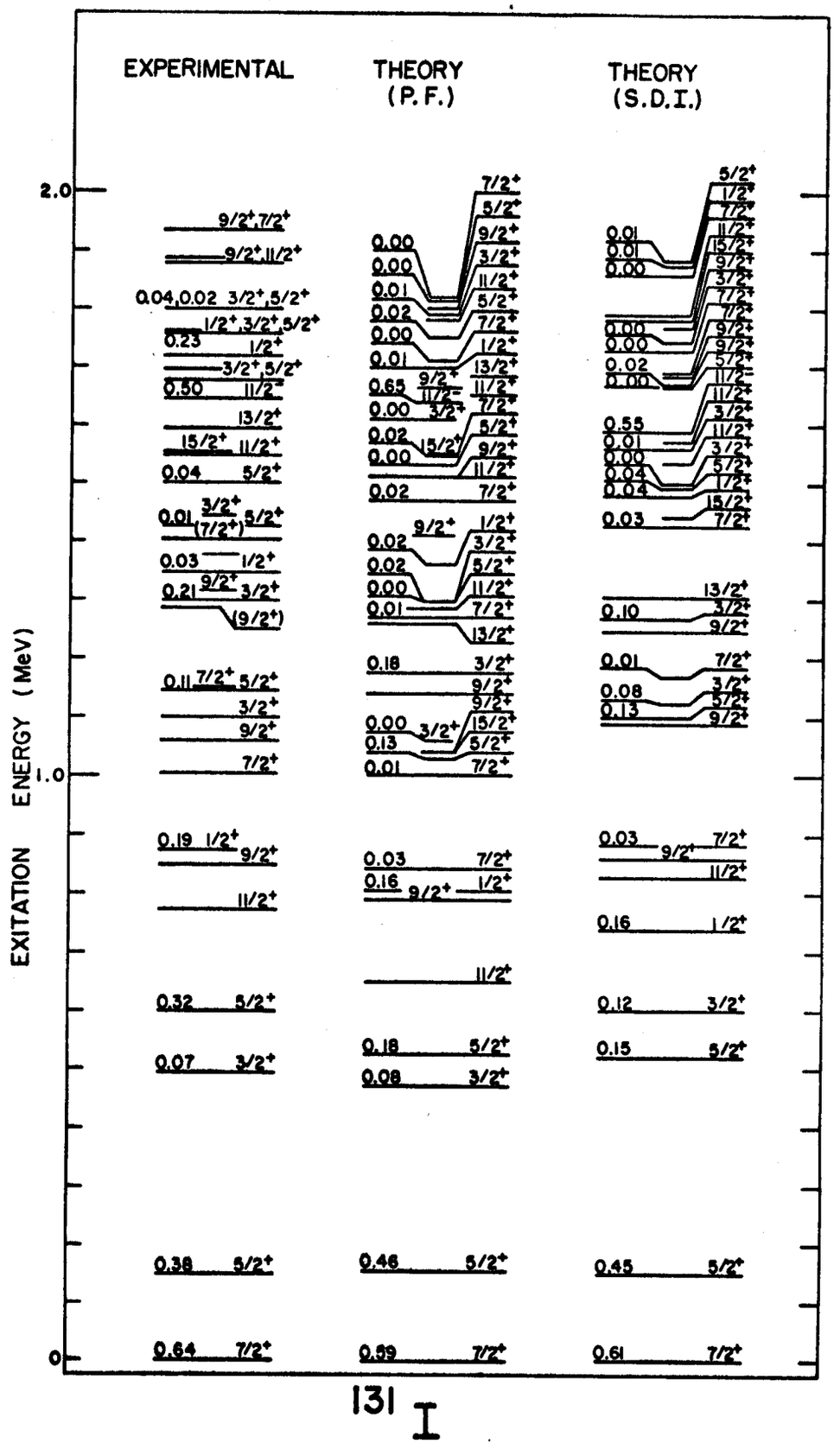
EXPERIMENTAL
THEORY (P.F.)
THEORY (S.D.I.)
EXITATION ENERGY (MeV)
2.0
1.0
0
9/2+,7/2+
9/2+,11/2+
0.04,0.02 3/2+,5/2+
1/2+,3/2+,5/2+
0.23 1/2+
3/2+,5/2+
0.50 11/2-
13/2+
15/2+ 11/2+
0.04 5/2+
0.01 3/2+ 5/2+
(7/2+)
0.03 1/2+
0.21 9/2+ 3/2+
(9/2+)
0.11 7/2+ 5/2+
3/2+
9/2+
7/2+
0.19 1/2+ 9/2+
11/2+
0.32 5/2+
0.07 3/2+
0.38 5/2+
0.64 7/2+
0.46 5/2+
0.59 7/2+
0.45 5/2+
0.61 7/2+
131 I

FIGURE 5

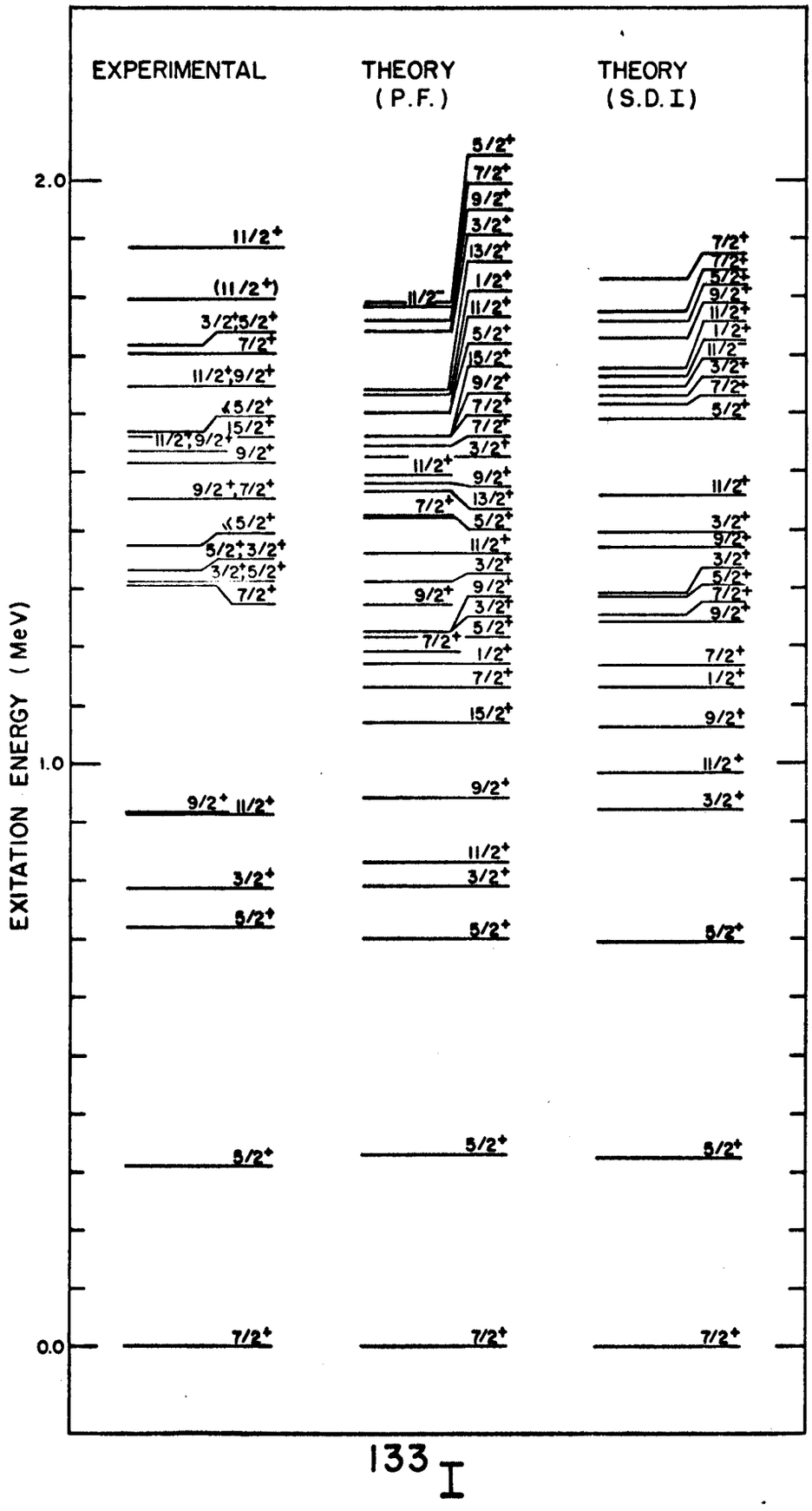

^{133}I

FIGURE 6